Hindawi
Scientific Programming
Volume 2022, Article ID 4414093, 14 pages
https://doi.org/10.1155/2022/4414093

Research Article

Substation Equipment Temperature Prediction Method considering Local Spatiotemporal Relationship

Lijie Sun,[1] **Shuang Chen**,[2] **Junfei Zhu**,[3] **and Jianhua Li**[1]

[1]*School of Electronics and Information Engineering, Taizhou University, Taizhou 318000, Zhejiang, China*
[2]*School of Aeronautical Engineering, Taizhou University, Taizhou 318000, Zhejiang, China*
[3]*State Grid Taizhou Power Supply Company, Taizhou 317700, Zhejiang, China*

Correspondence should be addressed to Shuang Chen; shuangchen@tzc.edu.cn

Received 17 June 2022; Accepted 29 July 2022; Published 24 August 2022

Academic Editor: Hongguang Ma

Temperature prediction of substation equipment is one of the important means for intelligent inspection of substation equipment. However, there are still three challenges: (1) Limited extracted samples; (2) Typical nonlinearity, seasonality, and periodicity; (3) Changes in equipment and working conditions. To solve the problems above, a substation equipment temperature prediction method considering Spatio-temporal relationship (SETPM-CLSTR) is proposed. First, according to the time series of equipment temperature from two aspects of temporal and spatial, it is determined that the equipment temperature has seasonal, temporal, and spatial correlation; second, aiming at the problem that the spatial location correlation cannot be described quantitatively, grey relational analysis (GRA) is adopted to determine the spatial location monitoring points closely related to the prediction target; then, the daily maximum temperature and daily minimum temperature from the environment, the predicted target temperature from the past several times in time and the temperature from the spatial location monitoring point with close correlation in space are constructed as Spatio-temporal feature vectors; finally, CNN-BiLSTM double-layer depth network model is proposed to predict the equipment temperature. SETPM-CLSTR has applied to temperature prediction of phase A contact from primary equipment of a substation in Taizhou City, Zhejiang Province. Under the two prediction performance evaluation indexes of MASE and RMSE, compared with three correlation models of LSTM, BiLSTM, and CNN-LSTM from two aspects of different features and models, it is verified that SETPM-CLSTR in this study has better prediction performance.

1. Introduction

Since 2020, large-scale blackouts have occurred in Mumbai, India, Pakistan, and Texas, which has brought great impact and losses to local economic and social development [1]. The safe development of the power grid is related to national security development and is the "lifeline" to be firmly guarded. Power companies face a great test in ensuring the safe operation and reliable power supply of the power grid. At present, China's power system is developing towards ultra-high voltage (UHV) and large capacity. In addition, society puts forward higher requirements for power supply quality and reliability. Substation equipment is an important material basis for the intrinsic safety of the power grid and the first line of defense for the safety of a large power grid, and ensuring the safe operation of equipment is the top priority [2]. In the power system with large units, large capacity, and high voltage, how to ensure the safe and stable operation of power equipment and how to patrol and monitor the equipment have become important links in the equipment management and transformation of the power system. Monitoring the operation status of this equipment in real-time and giving a timely response mechanism can effectively prevent the occurrence of accidents caused by abnormal operation of equipment.

Online monitoring is mainly aimed at primary equipment, including circuit breaker, disconnector, grounding knife (knife switch), transformer, bus, switch cabinet, cable connector, etc., to conduct real-time monitoring on its key points. During the operation of this equipment, it is easy to

cause heating and increase the temperature of the equipment due to aging insulation, excessive voltage load during operation, a loose connection of joints, loose bolts at key points, oxidation and corrosion of conductor surface or excessive contact resistance of contact surface. If it is light, it will cause damage and burning of relevant electrical equipment, and then lead to substation operation failure; More importantly, it will lead to fire and safety accidents, resulting in huge economic losses and social impact on the substation. Therefore, it is very important to know the temperature of each piece of equipment in real-time.

In recent years, the thermal failure caused by excessive equipment temperature has caused the shutdown of electrical equipment in substations, large-scale power failure in nearby areas, and even serious fire accidents [3]. For example, a substation in Luoyang, Henan Province, caused over-voltage due to a cable grounding fault, resulting in the fire of the distribution cabinet, resulting in the shutdown of power generation equipment, the power failure of surrounding communities, and serious losses. Therefore, online real-time monitoring of the temperature condition of power equipment during operation and predicting the temperature in the future can prevent faults. At the same time, in order to promote the intellectualization, informatization, and digitization of substation management and meet the needs of social development, it is imperative to build and optimize the substation equipment temperature prediction and fault early warning management system.

However, there are still three challenges in substation equipment temperature prediction:

(1) Limited extracted samples. There are two main reasons for the small amount of historical equipment temperature data extracted. On the one hand, according to the common sense of substation operation, the equipment temperature will be affected by the load, but the load data and the substation are not in the same department, and the data submission process between them is complex, Therefore, it is difficult to obtain load data. On the other hand, the data storage space of an intelligent inspection system is insufficient. The substation intelligent inspection system is quite large, involving many aspects and a large amount of data. Therefore, the storage space will be cleared regularly, and the automatic clearing time is generally set to 1 year.

(2) Typical nonlinearity, seasonality, and periodicity. The temperature data of substation equipment is affected by the equipment itself and many other factors, such as climate, environment, load, and so on, and its internal variation is irregular, with typical nonlinearity and seasonality, which makes it challenging task to construct a reasonable prediction model.

(3) Changes in equipment and working conditions. Substations are usually built in remote rural areas far from the urban area. The existence of abnormal weather conditions such as climate, air and thunder, rain, and snow make it more difficult to accurately predict the equipment temperature.

At present, the research mainly focuses on the traditional statistical analysis methods and machine learning methods, using time series as input characteristics to predict the temperature of substation equipment. For example, the ARMA series model [4], random forest (RF) method [5], neural network [6], etc, in which used historical temperature data and ambient temperature to form time series as a feature vector. However, the traditional models of substation equipment temperature prediction ignore the spatial relationship information of equipment in the historical time, resulting in poor prediction accuracy. Therefore, it is particularly important to select what characteristics to characterize the temperature for prediction. Therefore, when solving the problem of substation equipment temperature prediction, inspired by references [7–11], from the perspective of environment and multi-objective thinking [12–14], this study carries out feature extraction for the construction of substation equipment temperature prediction model from the two aspects of time and space, from the three dimensions of the interaction between different monitoring points of equipment, the seasonal characteristics of the influence of ambient temperature on equipment temperature and the influence of equipment temperature at historical time on equipment future temperature [15].

However, the more features are not the better for the prediction results. To solve the problems above, this study applies the grey relational analysis (GRA) [16] to analyze the location correlation of substation equipment, calculates the correlation between temperatures at different test points, takes the ambient temperature as the seasonal influencing factor, and integrates the three types of data of equipment temperature in the past. In the prediction modeling stage, deep learning network is widely used in various research fields [17–19], and according to the existing research, Convolutional Neural Network (CNN) has strong advantages in depth feature extraction [20] and Long Short-term Memory Networks (LSTM) network is suitable for processing and predicting important events with relatively long interval and delay in time series [21]. However, there is still a problem when using LSTM for time series prediction modeling: it is unable to encode the information from back to front. Bidirectional LSTM (BiLSTM) is a sequence processing model, which is composed of two LSTMs: one receives input in the forward direction and the other receives input in the backward direction. BiLSTM effectively increases the amount of information available in the network [22, 23]. Based on the above research results, this study uses CNN-BiLSTM double-layer depth network and multivariate time series model to realize the temperature prediction of substation equipment. This is expected to achieve better prediction performance.

In short, for substation equipment temperature prediction, the study proposes a method considering a local Spatio-temporal relationship, which is organized as follows:

(i) Section 2 describes basic theories, including grey correlation degree, LSTM network, and CNN;

(ii) Section 3 introduces data sources, conducts a multivariate analysis of data;

(iii) Section 4 describes SETPM-CLSTR, including feature selection, spatial feature extraction based on GRA, double-layer depth network prediction model based on CNN-BiLSTM, comparative experiments, and analysis of prediction results;

(iv) The conclusions are covered in Section 5.

2. Methodology

2.1. GRA. Grey system theory [24] is the concept of grey correlation analysis of each subsystem proposed by Professor Deng Julong, which aims to find the numerical relationship between each subsystem (or factor) in the system through certain methods. Grey relational analysis (GRA) is a very active branch of grey system theory, which can provide quantitative measurement for the development and change trend of the system, and its basic idea is to toughen the original observation number of evaluation indexes, calculate the correlation coefficient and correlation degree, and sort the evaluation indexes according to the correlation degree. GRA is realized in the following five steps.

(1) Determine the formula of the reference sequence X_0 and comparison sequence X_i, which are described as the formula (1) and the formula (2):

$$X_0 = [X_0(1), X_0(2), \ldots, X_0(n)], \tag{1}$$

$$X_i = [X_i(1), X_i(2), \ldots, X_i(n)] \, (i = 0, 1, \ldots, m). \tag{2}$$

(2) The raw data is subject to unlimited tempering, and the average method is expressed as the formula:

$$X_i'(k) = \frac{X_i(k)}{X_i(l)} \, (k = 1, 2, \ldots, n; \; i = 0, 1, \ldots, n). \tag{3}$$

(3) Calculate the difference sequence, calculate the absolute value difference between the reference sequence and the comparison sequence, and find out the maximum value ΔMax and minimum value ΔMin:

$$\Delta_j(k) = \left| X_0'(k) - X_j'(k) \right| (k = 1, 2, \ldots, n; \; j = 0, 1, \ldots, m). \tag{4}$$

(4) Calculation the correlation coefficient by the formula:

$$\delta_j(k) = \frac{\Delta_{\min} + \rho \Delta_{\max}}{\Delta_j(k) + \rho \Delta_{\max}}, \tag{5}$$

where ρ is the resolution coefficient, between [0, 1]. Generally, the smaller ρ is, the stronger the resolution is. In this study, $\rho = 0.5$ is taken.

(5) Calculate the correlation degree by the formula (6) and sort from large to small:

$$R_j = \frac{1}{n} \sum_{k=1}^{N} \delta_j(k) \, (k = 1, 2, \ldots, n). \tag{6}$$

2.2. LSTM Deep Network

2.2.1. RNN. The traditional neural network has made many achievements in various fields, but it has one main disadvantage, that is, it can not do the temporal correlation of information [25]. Recurrent neural network (RNN) is a special neural network structure, which is based on the view that human cognition is based on past experience and memory and is different from DNN and CNN in that it not only considers the input of the previous moment but also endows the network with a "memory" function of the previous content. The cyclic structure of RNN is shown on the left side of the equal sign in Figure 1, in which the module A receives the input X_t and outputs the value h_t. The expanded view of the annular structure is shown on the right side of the equal sign in Figure 1, in which $X_0, X_1, X_2, \ldots, X_t$ are the input time series, and $h_0, h_1, h_2, \ldots, h_t$ are the output time series.

The cyclic structure allows information to be transferred from one network state to the next. and a recurrent neural network can be considered as multiple copies of the same network, and each network transmits a signal to its next network. Therefore, all recurrent neural networks are repetitive neural network chains. In the standard RNN, this repetitive sub-module has a very simple structure, such as a tanh layer, which is shown in Figure 2.

2.2.2. LSTM Network. Long short-term memory (LSTM) network is a special RNN, and it is an improved recurrent neural network, which can solve the problem that RNN cannot deal with long-distance dependence and is widely used in time series prediction [26]. Like RNN, the LSTM network also has a chain structure, but the repeated submodule structure is different from RNN. The chain structure of the LSTM network is shown in Figure 3. It not only has a single neural network layer but is cycled by a forgetting gate, input gate, and output gate in a special way. The forgetting gate refers to the retention degree of the previous moment of state information; the input gate determines the information update degree according to the input current information and the current unit state; the output gate is responsible for outputting specific memory from the unit structure at the current time.

Where the meanings are represented by all symbols in Figures 3 and 4, respectively.

In Figure 4, line symbols contain a vector from one node to another. The pink circle represents point-to-point operations, such as vector addition, and the yellow box represents the learned neural network. Intersecting lines represent information merging, and separated arrow lines represent information replication and splitting.

The hidden unit structure of the LSTM network can be expressed by formulas:

$$f_t = \sigma\left(W_f x_t + U_f h_{t-1} + b_f\right), \tag{7}$$

$$i_t = \sigma\left(W_i x_i + U_i h_{t-1} + b_i\right), \tag{8}$$

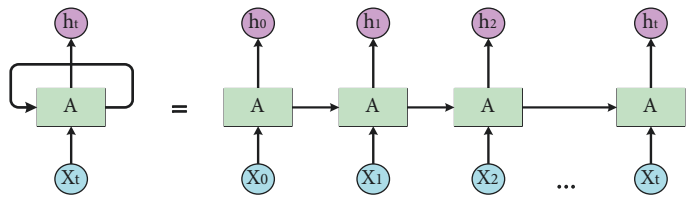

Figure 1: Cyclic structure and its expansion diagram of RNN.

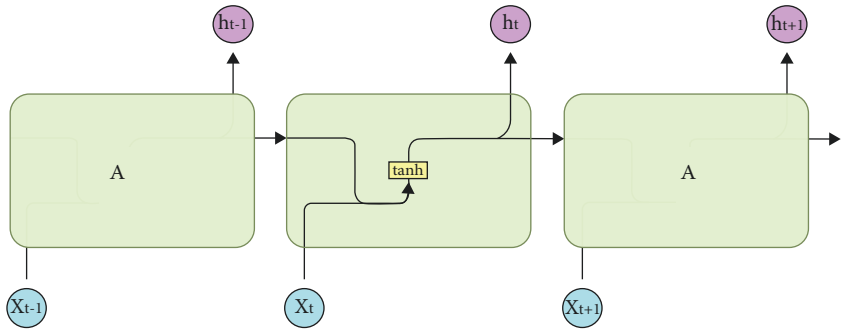

Figure 2: Sub module structure of RNN.

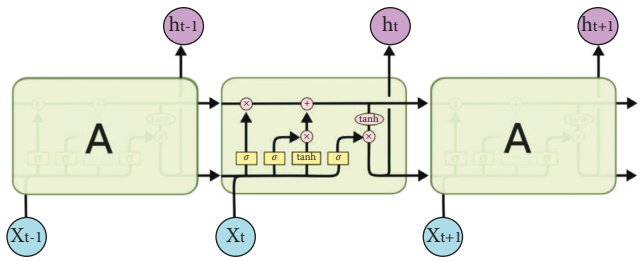

Figure 3: Sub module structure of LSTM.

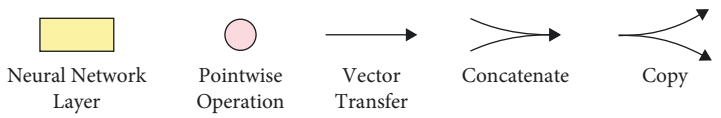

Figure 4: Schematic diagram of all symbols in Figure 3.

$$\tilde{c}_t = \tanh\left(W_c x_t + U_c h_{t-1} + b_c\right), \tag{9}$$

$$c_t = i_t \odot \tilde{c}_t + f_t \odot c_{t-1}, \tag{10}$$

$$o_t = \sigma\left(W_o x_t + U_o h_{t-1} + b_o\right), \tag{11}$$

$$h_t = o_t \odot \tanh\left(c_t\right), \tag{12}$$

where f_t and i_t respectively represent the forgetting gate and the input gate; $\tilde{c}_t$ and c_t respectively represent the candidate state and the unit state; o_t and h_t respectively represent the output gate and the final unit output; $W_f, U_f, b_f, w_i, U_i, b_i$, W_c, U_c, b_c, W_o, U_o and b_o are training parameter matrices; $\odot$ refers to Hadamard product.

2.3. CNN. Convolutional Neural Network (CNN) is one of the representative algorithms of deep learning. The basic structure of CNN is generally composed of the input layer, convolution layer, pooling layer, full connection layer, and output layer, in which the convolution layer and pooling layer are hidden layers [25]. In this study, CNN with three layers of convolution is used to characterize the temperature-depth of substation equipment, and the structure of CNN is shown in Figure 5.

In the convolution layer, each output feature map can combine and convolute the values of multiple feature maps, which are expressed as the formula:

$$x_j^l = f\left(u_j^l\right), \tag{13}$$

$$u_j^l = \sum_{i \in M_j} x_i^{l-1} * k_{ij}^l + b_j^l, \tag{14}$$

where u_j^l is the net activation of the j – th channel from the convolution layer l; M_j refers to the input characteristic graph subset of calculating net activation; k_{ij}^l and b_j^l represent the offset of convolution kernel matrix and

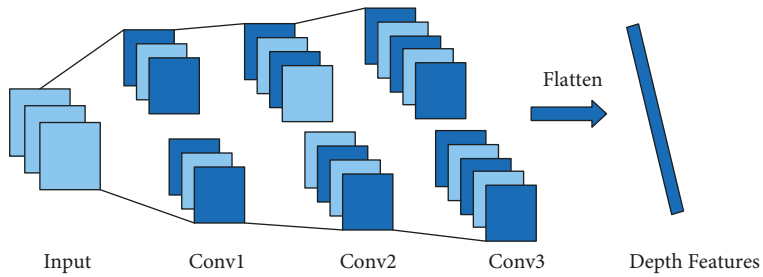

Figure 5: Structure diagram of CNN.

convoluted characteristic graph respectively; $*$ is the convolution symbol.

3. Problem Analysis

3.1. Description of Research Object. In January 2020, in order to promote the work deployment related to the ubiquitous power Internet of things of State Grid Corporation of China, promote the construction of intelligent deep supply, and jointly complete the intelligent inspection in the substation through a variety of high-tech means, so as to realize the intelligent automatic inspection in the substation instead of manual inspection, State Grid Zhejiang Electric Power Co., Ltd. specially formulated the pilot construction scheme of joint automatic inspection of high-definition video and intelligent inspection robot in the substation of Zhejiang Electric Power Co., Ltd. In response to this call, State Grid Companies in various cities in Zhejiang Province began to focus on establishing a joint automatic inspection system of substation high-definition video and intelligent inspection robot, so as to realize information connection, improve the joint intelligent inspection strategy, and expand the inspection functions of high-definition video and intelligent inspection robot.

The robot infrared temperature measurement subsystem is a functional branch of the video inspection system, which mainly aims at the infrared temperature measurement in the main transformer area, realizes the key temperature measurement monitoring of key equipment, sets the temperature measurement points of multi-point, multi-line, and multi-surface for the main transformer equipment, measures the temperature in real-time at the moving point of the mouse in the whole picture, and measures the temperature at multiple points in the whole picture at the same time. Moreover, the synchronous control function of the visible light camera makes the temperature measurement points more accurate. The outdoor robot inspection system can complete automatic inspection, remote inspection and special inspection tasks, and can replace personnel for daily inspection of equipment. Figure 6 shows that the wheeled robot in a substation in Taizhou is performing the task of infrared temperature measurement, the infrared imaging diagram of substation equipment is shown as the subgraph (a) in Figure 7, and the substation equipment diagram under visible light is shown as the subgraph (b) in Figure 7. The combined application of robot and physical identification (ID) adopts patrol correlation so that all abnormal data identified by the robot can be associated with the correct equipment. The goal of associating physical ID is to reverse write defects into the PMS system through physical ID information.

Figure 6: Process diagram of robot executing infrared temperature measurement task.

3.2. Data Acquisition. At present, the temperature early warning based on robot infrared temperature measurement is still in the trial operation stage, because the substation equipment is a large equipment, and there are many monitoring points and huge data. From the perspective of storage space and management, the initial inspection cycle of the robot is only set once a week, the shortest cycle is once a day, and there will be an interruption in the middle. Therefore, there is a serious practical problem that the early warning is not timely based on the robot's infrared temperature measurement to realize the equipment fault early warning task. Therefore, this study plays an important role in the equipment fault early warning based on the equipment temperature prediction.

The equipment of data acquisition is the primary equipment of the No. 2 main transformer from a 220 kV substation in Taizhou City, Zhejiang Province, and the temperature data is collected from October 1, 2019 to October 29, 2020 in this study, namely the data of 13 months. The primary equipment of the No. 2 main transformer consists of a 110 kV side and 220 kV side, and Table 1 shows the basic information of the equipment and the names of key points of equipment temperature inspection.

(a) (b)

Figure 7: Substation equipment diagram. (a) Infrared imaging diagram. (b) Substation equipment diagram of substation equipment under visible light.

Table 1: Summary of names for the equipment temperature monitoring key points.

Serial number	Equipment name
1	1–10 heat sinks at 220 side
2	19–23 heat sinks at 110 side
3	13–17 heat sinks at 110 side
4	110 side conservator
5	110 kV bushing phase C contact
6	110 kV bushing phase B contact
7	110 kV bushing phase A contact
8	220 kV bushing phase C contact
9	220 kV bushing phase B contact
10	220 kV bushing phase A contact
11	110 side equipment panorama
12	220 side equipment panorama

An intelligent inspection system is applied in the substation. The infrared equipment measures the temperature at 3 p.m. every day. The temperature data is exported in word form, that is, a multi-dimensional intelligent inspection report. The temperature data for more than a year is about 4G. The data in the database includes the name of key points of monitoring equipment, inspection time, inspection parts, inspection value (that is, the temperature value of key points of each equipment), temperature difference, infrared thermal imaging picture, alarm level manual review and description (fault description). In this study, the temperature monitored by 220 kV bushing phase A contact of No. 2 main transformer is selected for the experiment, including 370 days of data, the first 90% of the data set is used as the training set, and the remaining 10% of the data set is used as the test set.

3.3. Data Analysis

(1) Comparative analysis of the same equipment and the same monitoring point in different seasons.

According to the meteorological division method, in the meteorological department, usually, March to May of the Gregorian calendar is spring, June to August is summer, September to November is autumn, December to February of the next year is winter, and January, April, July, and October are often regarded as the representative months of winter, spring, summer, and autumn. Taking winter and summer as an example, this study analyzes the seasonal characteristics of substation equipment temperature, and Figure 8 shows the temperature change trend of phase A contact monitoring point of the bushing of No. 2 main transformer in Substation in winter and summer. Obviously, the average temperature of phase a contact is 30°C in winter and 50°C in summer. With the seasonal change, the equipment temperature changes significantly, which has an obvious positive correlation. Therefore, when predicting the equipment temperature, it is necessary to consider the ambient temperature factor.

(2) Comparative analysis of temperature at different monitoring points in the space-related position of the same equipment.

The primary equipment of the No. 2 main transformer consists of a 110 kV side and 220 kV side, and both sides of the equipment are independent of each other and have no intersection. Therefore, this study only analyzes the 220 kV side monitoring point where the phase A contact of the bushing is located for correlation analysis. The temperature trend diagram of 14 monitoring points at the 220 kV side is shown in Figure 9.

As can be seen from Figure 9, the temperatures at different monitoring points on the same side of the same equipment have a consistent trend and a typical linear correlation. There is a close relationship between the temperatures at most of the monitoring points. Therefore, it is necessary to consider spatial-related factors when predicting the temperature.

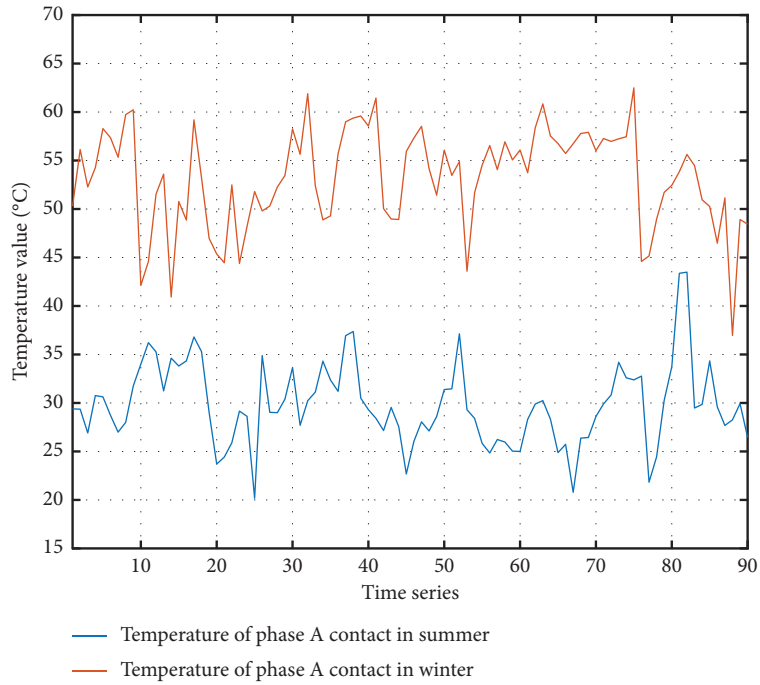

Figure 8: Seasonal trend chart of substation equipment temperature.

4. SETPM-CLSTR

According to the temperature data analysis for primary equipment of substation No. 2 main transformer in Section 3 of the previous article, the intelligent inspection of a substation based on a robot has the problems of long inspection cycle, short operation time and complex working environment, which lead that the substation equipment temperature prediction task has the characteristics of less characteristic parameters, small amount of data, instability, and seasonality. Based on the above problems, a substation equipment temperature prediction method considering local space-time relationship is proposed (recorded as SETPM-CLSTR), which is mainly realized through three links: feature selection, spatial feature extraction based on GRA, and double-layer depth network prediction model based on CNN-BiLSTM.

4.1. Feature Selection. For the task of substation equipment temperature prediction, the existing research only selects the characteristics of time, including the historical equipment temperature, and the daily maximum temperature and daily minimum temperature representing climate factors. This paper excavates the characteristics of space and establishes the feature vectors of space and time. In terms of time, the historical temperature data of several equipment-monitoring points and the daily maximum temperature and daily minimum temperature of the day are selected. In terms of space, the temperatures of all monitoring points on the same side of the equipment where the predicted target monitoring point is located are selected to form a Spatio-temporal feature set. Figure 10 shows the construction block diagram of the Spatio-temporal feature set.

4.2. Spatial Feature Extraction Based on GRA. The research object of this study is the primary equipment of the No. 2 main transformer in the substation. There are 14 monitoring points in 220 kV side space, one is the prediction target and 13 are the monitoring points related to spatial location. According to the spatial correlation analysis of the data in Chapter 3.3, it can be seen that different monitoring points have different correlation degrees with the prediction target, and the performance of the prediction model can not reach the best when the temperatures of all spatial monitoring points are used as spatial features. On the contrary, the existence of too many features with poor correlation will reduce the prediction performance of the model. Therefore, this study takes the temperature of phase A contact from bushing as the prediction target. In order to determine the monitoring points with high spatial correlation with phase A contact of bushing, this study uses GRA to calculate the grey correlation degree and quantitatively describe the contribution of the temperature of the monitoring point at the position of spatial correlation to the prediction target temperature, that is, calculate the correlation degree between the temperature of other 13 monitoring points and the temperature of phase A contact from the bushing. The greater the correlation degree, the higher the contribution to the prediction of phase A contact temperature of bushing, and the more it can characterize the temperature of phase A contact. Finally, the correlation degree is sorted in descending order. Grey correlation degree of temperature at local spatial correlation monitoring points at 220 kV side of the equipment is listed in Table 2.

According to the data in Table 2, this study selects the temperatures of the five spatial correlation monitoring points with the highest correlation degree as the spatial features, including phase B contact (recorded as B), phase C contact (recorded as C), No. 1 heat sink (recorded as 1#), No.

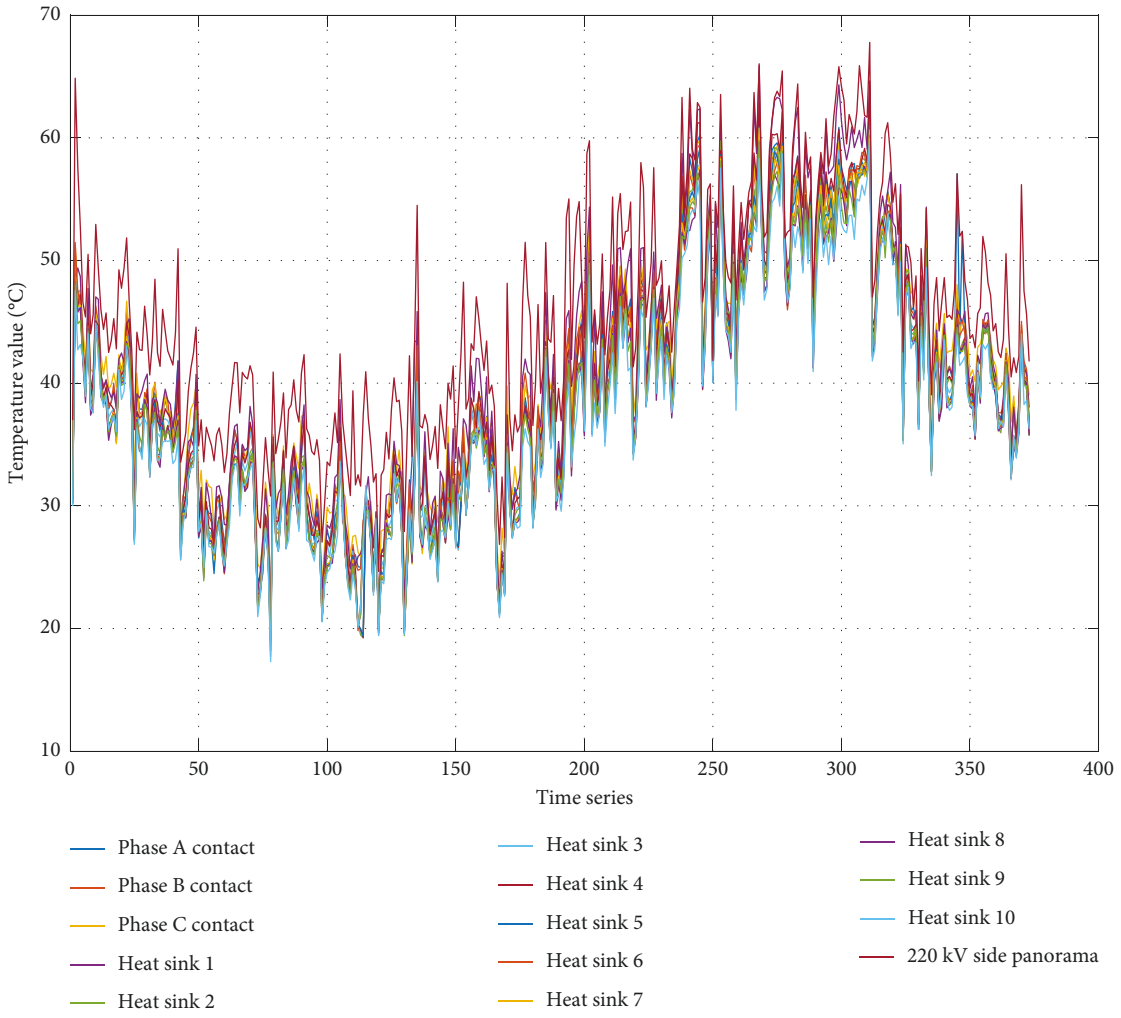

Figure 9: Temperature trend diagram of 14 monitoring points on 220 kV side.

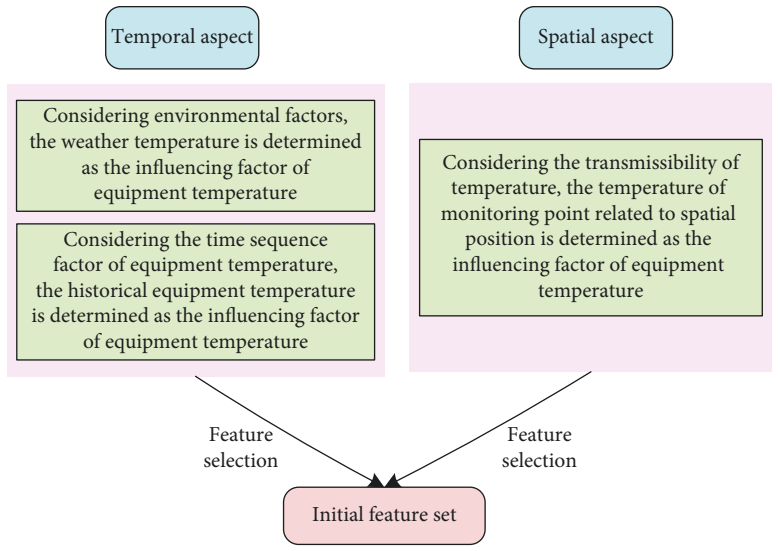

Figure 10: The construction block diagram of the Spatio-temporal feature set.

Table 2: Statistical table of grey correlation degree.

Local space location name	Correlation degree	Descending sort sequence number
220 kV bushing phase A contact	1	Prediction target (not sorted)
220 kV bushing phase B contact	0.9551	1
220 kV bushing phase C contact	0.9042	3
1# heat sink	0.8893	5
2# heat sink	0.8774	6
3# heat sink	0.8928	4
4# heat sink	0.9224	2
5# heat sink	0.8587	7
6# heat sink	0.8498	9
7# heat sink	0.8555	8
8# heat sink	0.8329	11
9# heat sink	0.8451	10
10# heat sink	0.8073	12
220 side equipment panorama	0.6657	13

Table 3: Partial samples of feature vector based on local Spatio-temporal relationship.

	Spatial features					Temporal features				
						Ambient characteristics		Historical temperature		
	B	C	1#	3#	4#	$D_{\max}$	$D_{\min}$	$T(t-1)$	$T(t-2)$	$T(t-3)$
1	47.55	47.21	47.62	48.69	46.67	52.70	31	22	47.41	48.90
2	42.64	42.68	44.51	42.82	42.23	46.58	30	20	47.55	47.41
3	39.95	40.37	41.76	39.92	39.13	45.40	25	18	42.64	47.55
...	...	...	...	...	...	...	...	...	...	...
370	51.79	50.72	51.37	54.35	51.63	54.22	21	18	46.06	47.97

3 heat sink (recorded as 1#) and No. 4 heat sink (recorded as 1#), selects the daily highest temperature (recorded as $D_{\max}$) and daily lowest temperature (recorded as $D_{\min}$) as the ambient characteristics, and selects the temperature of phase A contact in the first three days as the temporal features (recorded as $T(t-1)$, $T(t-2)$, $T(t-3)$ respectively), namely, the feature vector consists of 10 features based on local Spatio-temporal relationship, and some samples are shown in Table 3.

4.3. Normalization Processing. There is no comparability between the features of the feature vector based on the local Spatio-temporal relationship; therefore, normalization is needed before establishing the prediction model. Max − Min normalization method is used in this study, which is expressed as the formula:

$$X^* = \frac{X - \min}{\max - \min}, \tag{15}$$

where X is the temperature value; X^* is the value after Normalization processing; max is the maximum value of sample data, and min is the minimum value of sample data.

4.4. Double Layer Depth Network Prediction Model Based on CNN-BiLSTM. At this stage, it is necessary to establish a prediction model for substation equipment temperature prediction. This study proposes to use CNN and BiLSTM to build a two-layer depth network prediction model [26]. CNN is the depth feature extraction layer to mine the depth features of the feature vector based on the local space-time relationship after normalization, so as to obtain more information that can characterize the temperature of the predicted target monitoring point. BiLSTM is a bidirectional long and short memory depth network prediction layer to realize the regression prediction of substation equipment temperature.

BiLSTM is the abbreviation of Bi-directional Long Short-Term Memory, which is the combination of forwarding LSTM and backward LSTM, and both LSTM networks are connected to an output layer. This structure provides complete past and future time information for each point in the input sequence of the output layer. The BiLSTM network structure is shown in Figure 11, in which D_t represents the input of the network, refers to the temperature-depth characteristics of substation equipment extracted by CNN in this study; Y_t represents the output of the network, and refers the temperature prediction output of substation equipment in this paper.

4.5. The Implementation Process of SETPM-CLSTR. According to the above description, the specific implementation process of SETPM-CLSTR can be completed in the following five steps:

(1) According to the collected substation equipment temperature data and ambient temperature data, from the two aspects of time and space, the Spatio-

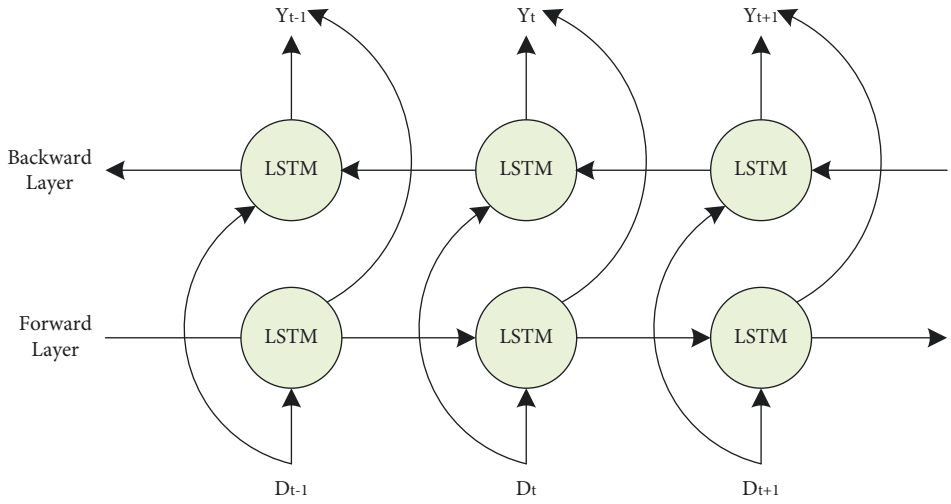

Figure 11: BiLSTM network structure.

temporal feature set is established under the three dimensions of equipment historical temperature, ambient temperature, and spatial local correlation monitoring point temperature.

(2) The grey correlation analysis method is used to analyze the spatial characteristics, determine the closely related spatial location related monitoring points, and combine n_1 historical past temperature of equipment, n_2 closely related temperature of spatial location monitoring points, the daily maximum and minimum temperature to form the feature vector based on local Spatio-temporal relationship;

(3) CNN is applied to extract the depth feature of the feature vector based on the local Spatio-temporal relationship to obtain the depth feature vector.

(4) Train BiLSTM depth network model with training set;

(5) For the test set, the trained BiLSTM model is applied to predict the temperature of substation equipment, and the prediction results are output.

The implementation process of SETPM-CLSTR is shown in Figure 12.

4.6. Temperature Prediction of Substation Equipment Based on CNN-BiLSTM

4.6.1. Specific Implementation Details of the Temperature Prediction. In this study, the CNN-BiLSTM network is used to predict the phase A contact of bushing, where, the CNN filter size is 10; the training cycle is 24 times per round, 60 rounds in total, and the total number of iterations is 1440; the learning rate is 0.005 and the error threshold is 0.001; The input of BiLSTM network is 128, the output is 32, and a full connection is added to get a temperature prediction value.

The prediction results for the test set based on CNN-BiLSTM are shown in Figure 13, and the testing relative error is shown in Figure 14.

It can be seen that the prediction effect of bushing phase A contact temperature based on the CNN-BiLSTM network is good, the main trend of the predicted value and the real value is basically consistent, and the relative error remains between $[-0.02, 0.04]$ in the test set from Figure 14, and this error range is acceptable and can meet the prediction accuracy requirements of substation equipment temperature early warning.

4.6.2. Prediction Performance Evaluation Indexes. In this study, mean absolute percentage error (MAPE) and root mean square error (RMSE) are used as the evaluation indexes of the prediction effect of the model [27, 28], and the calculation formula is shown in formula (16) and formula (17), respectively:

$$\delta_{\text{MAPE}} = \frac{1}{n}\sum_{r=1}^{n}\frac{\left|y_r - \widehat{y}_r\right|}{y_r} \times 100\%, \tag{16}$$

where n represents the number of prediction; y_r is the $r-$th real value of the temperature; $\widehat{y}_r$ is the $r-$th prediction of the temperature; the range of MAPE value is $[0, +\infty)$, the greater the error, the greater the value, therefore, the smaller the value, the better the performance.

$$\delta_{\text{RMSE}} = \sqrt{\frac{1}{n}\sum_{r=1}^{n}\left(y_r - \widehat{y}_r\right)^2}, \tag{17}$$

where n, y_r and $\widehat{y}_r$ have the same means with formula (16). The range of RMSE value is $[0, +\infty)$, the greater the error, the greater the value, and when the predicted value is completely consistent with the real value, RMSE = 0, namely, the perfect model.

4.6.3. Comparative Experiments. In order to verify the effectiveness of the method proposed in this study, two comparative experiments are carried out. On the one hand, to verify that the local Spatio-temporal relationship features are more effective than all features; On the other hand, it verifies the effectiveness of the CNN-BiLSTM double-layer depth network

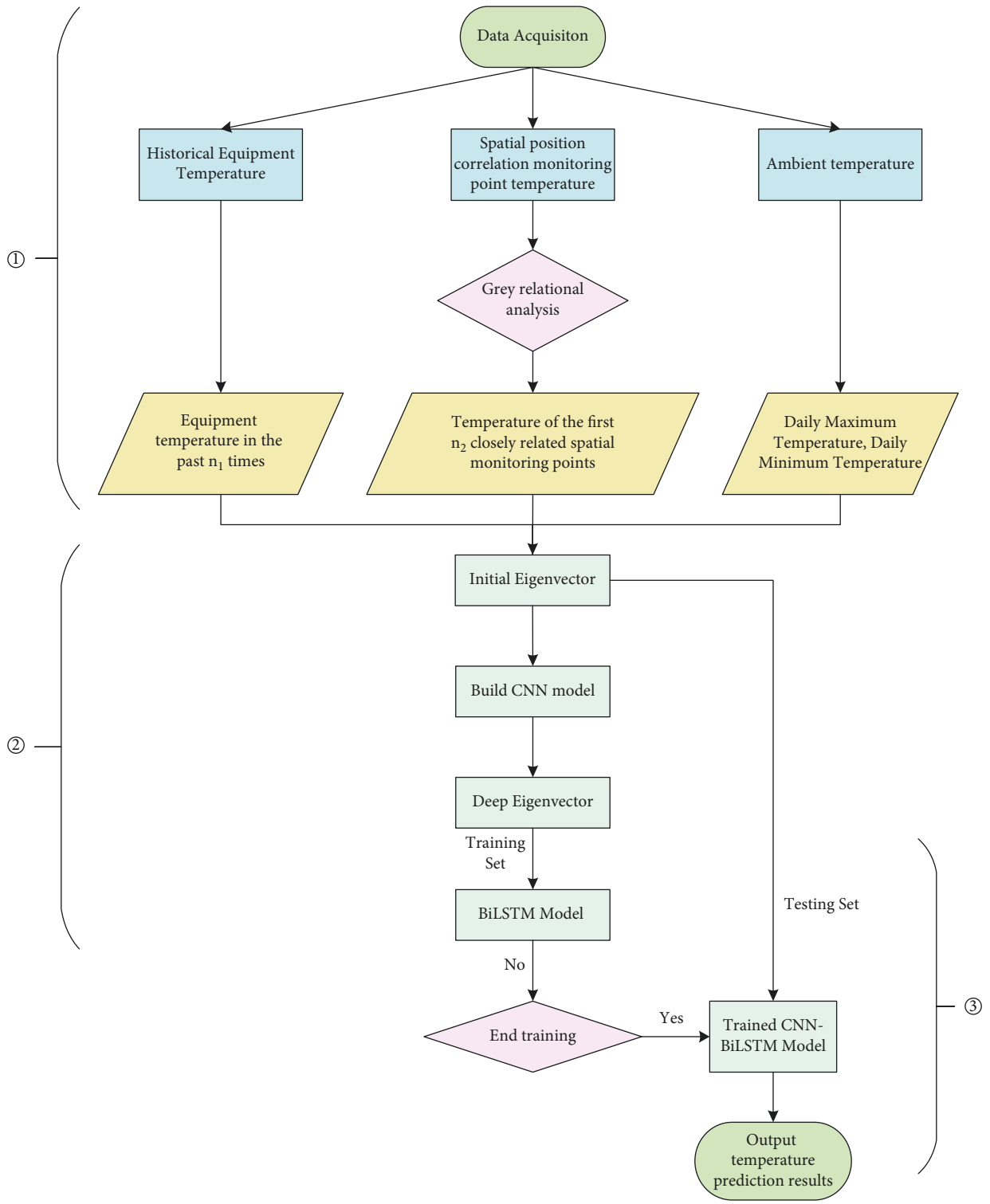

① Constructing feature vector based on local spatio-temporal relationship, which includes n_1 historical temperature data of the equipment, the temperature of the first n_2 closely related spatial monitoring points obtained by using the grey correlation analysis method, dAily maximum temperature and daily minimum temperature;

② Train CNN-BiLSTM network Model: CNN is applied to extract the depth feature of the feature vector, and BiLSTM network is used to predict the temperature of the equipment;

③ Network moDel test: test the performance of the trained CNN-BiLSTM model and output the predicted temperature of substation equipmtnt.

Figure 12: The implementation process of SETPM-CLSTR.

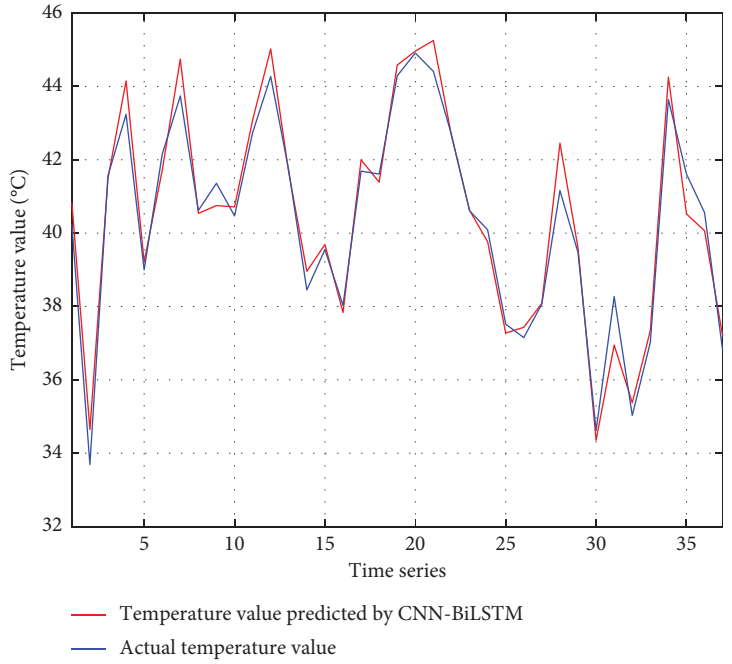

Figure 13: The prediction results for test set based on CNN-BiLSTM.

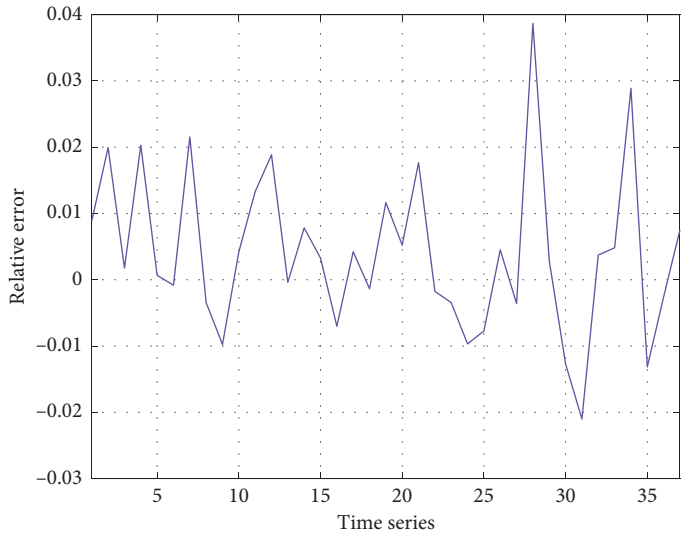

Figure 14: The testing relative error based on CNN-BiLSTM.

Table 4: Comparison results of prediction performance of different models.

Model	All features (18 dimensions)		CLSTR features (10 dimensions)	
	MAPE	RMSE	MAPE	RMSE
CNN-BiLSTM	1.03	60.09	0.94	52.86
CNN-LSTM	1.43	82.03	1.04	61.28
BiLSTM	5.77	634.74	5.47	552.96
LSTM	6.52	720.51	6.27	697.46

model in prediction performance. The comparison results of prediction performance are shown in Table 4. All features (18 dimensions) include two environmental characteristics of the daily maximum temperature and daily minimum temperature, the historical equipment temperature in the past three times and the temperature of 13 spatial location correlation monitoring points, a total of 18 characteristics, and CLSTR features refer to 10 features proposed in this study.

4.6.4. Analysis of Prediction Results. According to the above comparative experiments, this paper analyzes the prediction results according to the statistical results from Table 4:

(1) Under four models, CLSTR features proposed by this study have better performance than all features, which shows that when predicting the temperature of substation equipment, the more parameters, the better the prediction performance of the model;

(2) The model using CNN for depth feature extraction, including the CNN-BiLSTM network and the CNN-LSTM network, has significantly improved the prediction performance compared with the model without CNN(BiLSTM and LSTM), which shows that CNN plays a vital role in the temperature feature extraction of substation equipment.

(3) From the two aspects of feature extraction and combined modeling, the proposed SETPM-CLSTR has significantly improved the temperature prediction performance of substation equipment. Under the two evaluation indexes of MAPE and RMSE, this method has the best prediction performance compared with the other three models.

5. Conclusions

In order to ensure the stable operation of the power grid system and the safe operation of power equipment, an intelligent inspection system is gradually adopted in substations. Temperature early warning based on substation equipment is one of the main branches. Aiming at the difficulties of robot infrared temperature prediction in three aspects: less data, seasonality, and a complex working environment, SETPM-CLSTR is proposed in this study. Using the equipment temperature data of 220 kV side of No. 2 main transformer of a substation in Taizhou City, Zhejiang Province, comparative experiments are carried out in two aspects of different characteristics and different models. It is verified that the method proposed in this study has good prediction performance, and can provide a new idea for the temperature early warning system of intelligent patrol inspection of State Grid.

Although this research has achieved good prediction results, there is less research data in this study, and more research data should be collected in future research. The application of substation equipment temperature prediction for early equipment fault early warning is the content of future research [29, 30].

Data Availability

The equipment of data acquisition is the primary equipment of No. 2 main transformer from a 220 kV substation in Taizhou City, Zhejiang Province, and the temperature data is collected from October 1, 2019 to October 29, 2020 in this study, which can be obtained via e-mail to lijiesun@tzc.edu.cn.

Conflicts of Interest

The authors declare no conflicts of interest.

Authors' Contributions

Lijie Sun wrote the original draft, developed the methodology, helped with software, validated the study, and carried out the experiment. Shuang Chen visualized and investigated the study. Junfei Zhu wrote, reviewed, and edited the study, helped with software, and analysed the study. Jianhua Li supervised and editing the study and carried out typesetting.

Acknowledgments

This work was supported by Research Project of Education Department of Zhejiang Province (Y201840245).

References

[1] Y. Hu, S. Xue, H. Zhang et al., "Deep Cause Analysis and enlightenment of global blackout in recent 30 years," *China Electric Power*, vol. 4, no. 10, pp. 204–210, 2015.

[2] Y. Xin, *Design and Implementation of On-Line Temperature Monitoring and Early Warning System for Power Equipment*, Shandong University, Jinan, China, 2013.

[3] Y. J. Lin, "Substation equipment operation failure causes and treatment countermeasures," *China's new technologies and products*, vol. 13, pp. 60-61, 2017.

[4] M. Baptista, S. Sankararaman, I. P. Medeiros, C. Nascimento, H. Prendinger, and E. M. Henriques, "Forecasting fault events for predictive maintenance using data-driven techniques and ARMA modeling," *Computers & Industrial Engineering*, vol. 115, pp. 41–53, 2018.

[5] C. k. Lei, J. Deng, K. Cao, L. Ma, Y. Xiao, and L. Ren, "A random forest approach for predicting coal spontaneous combustion," *Fuel*, vol. 223, pp. 63–73, 2018.

[6] X. H. Kong and H. F. Zhang, "Substation Equipment Temperature prediction based on optimized generalized regression neural network," *China Electric Power*, vol. 49, no. 7, pp. 54–59, 2016.

[7] X. F. Xu, Z. R. Lin, and J. Zhu, "DVRP with limited supply and variable neighborhood region in refined oil distribution," *Annals of Operations Research*, vol. 309, no. 2, pp. 663–687, 2022.

[8] Z. Tian, C. Luo, H. Lu, S. Su, Y. Sun, and M. Zhang, "User and entity behavior analysis under urban big data," *ACM/IMS Transactions on Data Science*, vol. 1, no. 3, p. 1, 2020.

[9] X. F. Xu, J. Hao, and Y. Zheng, "Multi-objective artificial bee colony algorithm for multi-stage resource leveling problem in sharing logistics network," *Computers & Industrial Engineering*, vol. 142, no. 4, Article ID 106338, 2020.

[10] J. Hou, F. Chen, P. Li, and Z. Zhu, "Gray-box parsimonious subspace identification of Hammerstein-type systems," *IEEE Transactions on Industrial Electronics*, vol. 68, no. 10, pp. 9941–9951, 2021.

[11] T. Yu, Q. Gan, G. Feng, and G. Han, "A new fuzzy cognitive maps classifier based on capsule network," *Knowledge-Based Systems*, vol. 250, Article ID 108950, 2022.

[12] X. F. Xu, Z. R. Lin, X. Li, C. J. Shang, and Q. Shen, "Multi-objective robust optimisation model for MDVRPLS in refined

oil distribution," *International Journal of Production Research*, vol. 5, pp. 1–21, 2021.

[13] Y. Z. Hao and H. L. He, "Application analysis of infrared temperature measurement technology in substation operation and maintenance," *Electrical materials*, vol. 6, pp. 70–72, 2021.

[14] X. F. Xu, C. L. Wang, and P. Zhou, "GVRP considered oil-gas recovery in refined oil distribution: from an environmental perspective," *International Journal of Production Economics*, vol. 235, Article ID 108078, 2021.

[15] Z. Tian, W. Shi, Y. Wang et al., "Real time lateral movement detection based on evidence reasoning network for edge computing environment," *IEEE Transactions on Industrial Informatics*, vol. 15, no. 7, pp. 4285–4294, 2019.

[16] Y. H. Kim, S. H. Nam, S. B. Hong, and K. R. Park, "GRA-GAN: g," *Expert Systems with Applications*, vol. 198, Article ID 116792, 2022.

[17] Z. Tian, C. Luo, J. Qiu, X. Du, and M. Guizani, "A distributed deep learning system for web attack detection on edge devices," *IEEE Transactions on Industrial Informatics*, vol. 16, no. 3, pp. 1963–1971, 2020.

[18] X. Gao, X. Li, B. Zhao, W. Ji, X. Jing, and Y. He, "Short-term electricity load forecasting model based on EMD-GRU with feature selection," *Energies*, vol. 12, no. 6, p. 1140, 2019.

[19] X. F. Xu and Y. Y. He, "Blockchain Application in Modern Logistics Information Sharing: A Review and Case Study Analysis," *Production Planning & Control*, vol. 107, 2022.

[20] J. Yin, C. Ning, and T. Tang, "Data-Driven Models for Train Control Dynamics in High-Speed Railways: LAG-LSTM for Train Trajectory Prediction," *Information Sciences*, vol. 600, pp. 377–400, 2022.

[21] K. Feng and Z. Fan, "A novel bidirectional LSTM network based on scale factor for atrial fibrillation signals classification," *Biomedical Signal Processing and Control*, vol. 76, Article ID 103663, 2022.

[22] Y. Wang, X. Jiang, F. Yan, Y. Cai, and S. Liao, "The GRA-two algorithm for massive-scale feature selection problem in power system scenario classification and prediction," *Energy Reports*, vol. 7, pp. 293–303, 2021.

[23] F. L. Yin, X. M. Xue, C. Z. Zhang et al., "Multifidelity genetic transfer: an efficient framework for production optimization," *SPE Journal*, vol. 26, no. 4, pp. 1614–1635, 2021.

[24] L. Wu and L. Noels, "Recurrent Neural Networks (RNNs) with dimensionality reduction and break down in computational mechanics application to multi-scale localization step," *Computer Methods in Applied Mechanics and Engineering*, vol. 390, Article ID 114476, 2022.

[25] Y. Zhang, C. Li, Y. Jiang et al., "Accurate prediction of water quality in urban drainage network with integrated EMD-LSTM model," *Journal of Cleaner Production*, vol. 354, Article ID 131724, 2022.

[26] L. Yang, C. Ma, H. Hu, and D. Huang, "Study on Regional Medium and long-term temperature prediction based on improved LSTMs model," *Journal of Huizhou College*, vol. 41, no. 6, pp. 75–79, 2021.

[27] X. F. Xu, W. Liu, and L. A. Yu, "Trajectory prediction for heterogeneous traffic-agents using knowledge correction data-driven model," *Information Sciences*, vol. 608, pp. 375–391, 2022.

[28] Y. Wang, C. Zhu, Y. Wang, J. Sun, D. Ling, and L. Wang, "Survival risk prediction model for ESCC based on relief feature selection and CNN," *Computers in Biology and Medicine*, vol. 145, Article ID 105460, 2022.

[29] Z. Liang, G. Q. Sun, H. C. Li et al., "Short-term load forecasting based on deep belief network optimized by VMD and PSO," *Grid Technology*, vol. 42, no. 2, pp. 598–606, 2018.

[30] K. Hu, Y. Wang, W. Li, and L. Wang, "CNN-BiLSTM enabled prediction on molten pool width for thin-walled part fabrication using Laser Directed Energy Deposition," *Journal of Manufacturing Processes*, vol. 78, pp. 32–45, 2022.